arXiv:cond-mat/0405641v1 [cond-mat.stat-mech] 27 May 2004

Off-lattice Kinetic Monte Carlo simulations of strained heteroepitaxial growth

Michael Biehl, Florian Much, and Christian Vey

Abstract. An off-lattice, continuous space Kinetic Monte Carlo (KMC) algorithm is discussed and applied in the investigation of strained heteroepitaxial crystal growth. As a starting point, we study a simplifying (1+1)-dimensional situation with inter-atomic interactions given by simple pair-potentials. The model exhibits the appearance of strain-induced misfit dislocations at a characteristic film thickness. In our KMC simulations we observe a power law dependence of this critical thickness on the lattice misfit, which is in agreement with experimental results for semiconductor compounds. We furthermore investigate the emergence of strain induced multilayer islands or *Dots* upon an adsorbate wetting layer in the so-called Stranski-Krastanow (SK) growth mode. At a characteristic kinetic film thickness, a transition from monolayer to multilayer island growth occurs. We discuss the microscopic causes of the SK-transition and its dependence on the model parameters, i.e. lattice misfit, growth rate, and substrate temperature.

1. Introduction

Atomistic models of crystal growth in Molecular Beam Epitaxy and similar techniques continue to attract considerable interest, see for example [1, 2, 3, 4] for overviews, a very brief introduction is given in [5], this volume. Many interesting aspects of epitaxial growth can be discussed for the case of homoepitaxy where only one material is present. This includes the deposition of, for instance, a metal or a semiconductor compound on a matching substrate crystal.

The term heteroepitaxial crystal growth refers to situations, where the deposited adsorbate material differs from the substrate. The mismatch can be quite fundamental, as for instance in the growth of organic films upon metal substrates. Perhaps the most frequent and, certainly, the conceptually simplest situation is that where adsorbate and substrate would crystallize in the same type of lattice, but with slightly different lattice spacings.

The latter case is of particular relevance in the fabrication of semiconductor heterostructures for potential technical applications, such as modern optoelectronic or storage devices. Prominent examples are the deposition of Ge on Si, InAs on GaAs, or CdTe on ZnSe. Frequently, the aim is to produce a smooth adsorbate film of a well defined thickness on a given substrate. However, the misfit induced strain can perturb the lattice structure and result in, e.g., dislocations which reduce the quality of the film drastically.

On the other hand, mechanisms of strain relaxation can also be exploited in epitaxial growth. The most prominent example is perhaps the self-organized formation of multilayered islands in the so–called Stranski-Krastanov growth mode [1]. The ideal process would yield dislocation-free three-dimensional objects of well defined size and shape which furthermore display spatial ordering. These so–called Quantum Dots can capture single or few electrons and may play the role of *artificial atoms* in a novel type of solid-state-lasers, for example. For a recent overview of the many interesting experimental and theoretical aspects of Quantum Dot physics, see [6].

Besides the obvious technological relevance of heteroepitaxial growth, it is also highly interesting from a theoretical point of view. The self-assembly of Dots might be considered a prototype example of self-organized ordering processes. Heteroepitaxy remains furthermore a challenge in the design of growth models and the development of novel simulation techniques.

The natural tool for mismatched heteroepitaxy appears to be Molecular Dynamics (MD) [7] or quantum mechanical variations thereof, e.g. [8]. This very attractive but computationally demanding approach is discussed in the general context of epitaxial growth in [9] (K. Albe, this volume), see [10] for an example application in the context of dislocation formation. Whereas modern computers allow for the simulation of very large systems, the most serious limitation of the MD technique remains: The physical time intervals that can be targeted are generally quite small, e.g. on the order of picoseconds. MBE relevant time scales of seconds or even minutes do not seem feasible currently, even when applying highly sophisticated acceleration techniques as in [11].

In simplifying lattice gas models, the particles can only be placed exactly at pre-defined sites. Nevertheless, it is possible to incorporate certain misfit effects into such models. In fact, some of the earliest KMC simulations were performed in the context of strained heteroepitaxial crystal growth [12]. So–called *ball and spring* models consider additional harmonic interactions, i.e. *springs*, between adsorbate or substrate atoms at neighboring lattice sites, see [12] and [13, 14] for more recent examples. In other approaches, continuum elasticity theory is applied to evaluate the contribution and influence of strain for a given configuration of the lattice [15] (and references therein).

However, traditional lattice based models cannot cope with the emergence of defects or dislocations in a straightforward fashion. In the following we will discuss an off-lattice model and the corresponding Kinetic Monte Carlo (KMC) technique, which allows for continuous particle positions and in which strain results directly

from the atomic interactions. Schindler and Wolf have essentially formulated the model and simulation method in [17, 18], and some of the results presented here have been published previously in [19, 20, 21]. For a detailed description of the concept and its applications see also [22].

The method incorporates the essential features of hetero-epitaxy in a natural way, and, at the same time, enables us to perform simulations over reasonable physical time scales. In contrast to earlier realizations of similar concepts, see e.g. [17, 18, 23, 24], we are also able to simulate the growth of rather thick films over a wide range of misfits.

In section 2 we will define the model and describe the simulation technique. We briefly discuss the role of misfit dislocations as a mechanism for strain relaxation and present our simulation results in section 3. Section 4 summarizes our investigations of the Stranski-Krastanov growth mode and in section 5 we conclude with a brief outlook on perspective investigations.

2. Model and method

In the following, we address quite fundamental and general aspects of heteroepitaxy, rather than the properties of specific material systems. Hence, the primary goal is to develop a fairly simple model which still captures the essential features of a mismatched growth situation.

Following several previous studies [17, 18, 23, 24], we choose a pair potential ansatz to model interactions between the particles. To begin with, we consider a Lennard-Jones (LJ) system [25]. A strong repulsive term at small distances competes with an attractive contribution in the potential

$$U_{ij}(U_o, \sigma) \;=\; 4\,U_o \left[\left(\tfrac{\sigma}{r_{ij}}\right)^{12} \;-\; \left(\tfrac{\sigma}{r_{ij}}\right)^{6} \right]. \tag{2.1}$$

The relative distance r_{ij} of particles i and j varies continuously with their position in space. By choice of the parameters U_o and σ we can specify the different material properties in our model: interactions between two substrate or adsorbate atoms are given by the sets $\{U_s, \sigma_s\}$ and $\{U_a, \sigma_a\}$, respectively. In principle, an independent set of parameters would define the interaction of substrate with adsorbate atoms. In order to keep the number of parameters small, we follow a standard approach and set $U_{as} = \sqrt{U_s U_a}, \sigma_{as} = (\sigma_s + \sigma_a)/2$ for the inter-species potential.

The potential energy of two isolated atoms that interact via (2.1) is minimal for $r_{ij} = 2^{1/6}\sigma$. Accordingly, the lattice spacing in a Lennard-Jones crystal is proportional (and close) to σ as well. The relative lattice misfit in our model is therefore directly controlled by choice of σ_s and σ_a:

$$\epsilon = (\sigma_a - \sigma_s)/\sigma_s. \tag{2.2}$$

Essential features and several principled questions can already be studied in the simplifying framework of (1+1)-dimensional growth, where particles are deposited on a one-dimensional surface. For the simulations presented here we have prepared,

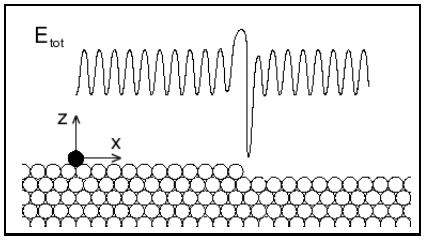


FIGURE 1. Illustration of the Molecular Statics calculations in $(1+1)$ dimensions. As the (black) adatom is virtually moved to the right, along the x-direction, the total energy of the system is locally minimized with respect to all other particle coordinates, including z for the moving adatom. The resulting potential energy surface displays an essentially periodic shape along the terraces and a pronounced Schwoebel barrier for moves across the edge.

at least, 6 layers of substrate particles, each containing L particles. The system sizes vary between $L = 200$ and $L = 800$ in the following, depending on the computational costs of the considered problem. We assume periodic boundary conditions in the lateral direction and fix the particle positions in the bottom layer in order to stabilize the crystal.

In our simulations of the growth kinetics, adsorbate particles are deposited at a constant rate R_d as measured in monolayers per second (ML/s). Desorption events will be completely suppressed here as they would be very unlikely anyway. Only adsorbate particles at the surface are considered mobile in the sense that they perform diffusion hops and the like. However, bulk crystal adsorbate and substrate atoms will be due to relaxation processes which modify their spatial positions and relative distances without changing the topology.

The most distinctive feature of the method is the treatment of thermally activated processes, for which we assume Arrhenius like rates, see [1, 2, 3, 5]. In lattice gas models, particles are moved from one site to another with a rate which usually depends on a small neighborhood only. In the off-lattice approach any event concerns the entire configuration and its rate depends on all particle coordinates, in principle. At a given time, the system resides in a local minimum of the total potential energy of the n particles:

$$E_{tot} = \sum_{i=1}^{n} \sum_{j=i+1}^{n} U_{ij}. \tag{2.3}$$

A possible event k takes the system to one of the neighboring minima in configuration space and for any such change the corresponding energy barrier E_k and rate R_k has to be evaluated by means of a so-called Molecular Statics calculation, see [16, 26] for examples and further references.

In a most general setting the identification of potential events, i.e. the relevant energy minima, can be difficult [26, 27, 28]. The $(1 + 1)$-dimensional situation simplifies these calculations to a large extent.

Figure 1 illustrates the procedure: The single particle on top of the terraced surface is virtually moved to the right, along the x-coordinate in the illustration. For every fixed value of x, the total energy (2.3) can be (locally) minimized with respect to the moving atom's z-coordinate and the positions of all other atoms including the substrate. In doing so, one can evaluate a potential energy surface (PES) as displayed in Fig. 1. Of course it is not necessary to scan the PES continuously for the Arrhenius rates, as only the energies in the initial state and the transition state are relevant. The latter corresponds to a maximum in the figure, i.e. a saddle point in the energy as a function of all coordinates. In more complex situations like $(2 + 1)$-dim. growth it is also possible to determine saddle points in a PES by iterative gradient based methods [22, 26, 27, 28]. However, the identification of the physical path from one minimum to the next can be much more involved in general, e.g. for concerted moves in $(2 + 1)$ dimensions.

Note that the $(1 + 1)$-dim. system displays a strong Ehrlich-Schwoebel effect [1, 2]: hops from a terrace are hindered by a barrier which relates to the very weakly bound transition state right at the edge. The effect is also present, but much weaker in a $(2 + 1)$-dim. fcc-system, for instance. There, a descending particle can follow a more favorable path *between* neighboring particles at the edge.

For large misfits, exchange processes at terrace or island edges may become more frequent than downward hopping diffusion. We have checked that for the values of ϵ considered in the following, exchange diffusion can be neglected, in general. The precise barriers, however, depend in a subtle way on the misfit, the island size, and the properties of the actual interaction potential. For details we refer to [22] and forthcoming publications.

Further simplifications may be used here. First, because the LJ-potential (2.1) is very weak for distances $r_{ij} > 3\sigma$, one can effectively cut-off the interactions and consider only particles in a corresponding neighborhood region when evaluating the PES of a particular event. The so-called *frozen crystal approximation* should be employed with care: in this scheme all coordinates but those of the moving atom are considered fixed, which significantly simplifies the saddle point search. Although the scheme appears to impose a drastic restriction, it has been reported by various authors that its main effect in the LJ-system is a uniform shift of all barriers by roughly 10% [16, 17, 18, 22].

In our simulations, exchange diffusion and multiple jumps have been neglected. We consider only hops to the left or right neighboring minimum in the PES. Given a configuration of the system, we set up a catalogue of all these diffusion events and evaluate their rates

$$R_k = \nu_o \exp\left[-\frac{E_k}{k_B T}\right] \qquad \text{with} \qquad \nu_o = 10^{12}/s \tag{2.4}$$

with E_k obtained as described above.

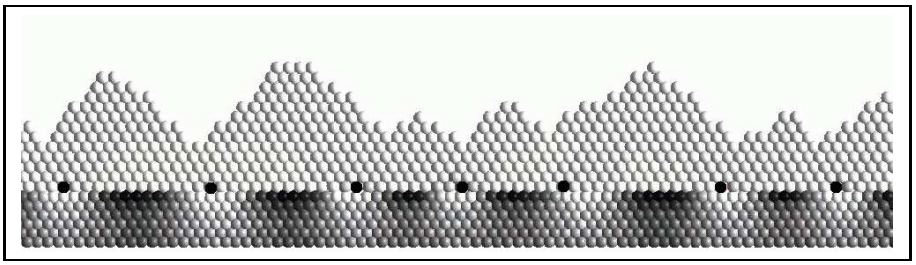


FIGURE 2. Dislocations: a film grown in the model without downhill funneling [19] for a large misfit of $\epsilon = +10\%$, section of a larger system with six layers of substrate. The lighter a particle is displayed, the smaller is its average distance to the nearest neighbors. Dislocations form right at the interface of adsorbate and substrate, as marked by the additional filled circles. Note that the elastic interaction with the film also affects the substrate.

For simplicity, we choose a constant pre-factor or *attempt frequency* ν_o for all diffusion processes, see [5] for a brief discussion and references. Next, one of the diffusion or deposition processes is chosen with a probability proportional to its rate. In order to facilitate an efficient book-keeping and fast search, events are stored in a binary search tree, see [3] and references therein. After performing the particular process, the catalogue of rates has to be updated and re-evaluated. Obviously this task consumes a large portion of the computing power. Nevertheless, the rejection-free method is advantageous over a rejection-based simulation [5].

Approximations and numerical inaccuracies, and even more so the use of the *frozen crystal* picture, result in deformations of the crystal and the accumulation of artificial strain energy. In order to avoid this effect, a relaxation of the system should be performed after each event, in the sense that the configuration is taken to the nearest local minimum of E_{tot}. In practice we perform after each diffusion or deposition a *local* relaxation within a radius 3σ about the location of the event. The full *global* procedure is applied only after a certain number of events, which is decreased whenever the relaxation changes the barriers by more than, say, a few percent.

In the following sections we discuss applications in the context of two different mechanisms of strain relaxation. Their peculiarities require certain extensions and modifications. However, the basic concepts and essential ingredients have been outlined above.

3. Formation of dislocations

If the misfit is relatively small in heteroepitaxial growth, one frequently observes the initial growth of a *pseudomorphic* film. Here the substrate determines the

lateral lattice constant also in the adsorbate and strain energy accumulates in the growing film. On the other hand, for very thick adsorbate films far away from the substrate, one clearly expects to find a lattice structure and spacing as in the undisturbed bulk material. The ultimate relaxation of strain is through misfit dislocations, lattice defects which allow the adsorbate to assume its natural lattice structure, eventually. Here we address the question of how the transition from strained pseudomorphic to relaxed adsorbate growth occurs and how the lattice spacing evolves with the film thickness.

In the frame of our model we choose the same potential depth for all types of interactions, which defines the energy scale. By identifying $U_a = U_s = U_{as}$ with the value $U_o = 1.3125eV$, for instance, we obtain a barrier of $0.90eV$ for surface diffusion in the case of zero misfit. The substrate temperature was set to $T = 0.03U_o/k_B \approx 460K$ which is well below the melting temperature of a monoatomic Lennard-Jones crystal. All results presented in this section were obtained with the deposition rate $R_d = 1ML/s$.

Dislocations can be identified by constructing Voronoy polyhedra and searching for particles with a coordination number different from six in the bulk. Further information is obtained from a Burgers construction, see [19, 22] for details.

In our earlier investigations presented in [19] we considered positive and negative values of the misfit parameter in the range $-15\% \leq \epsilon \leq +11\%$. For large absolute values of ϵ the system displays the formation of misfit dislocations right at or very close to the substrate/adsorbate interface, cf. Fig. 2. The slightly oversimplifying picture is that, initially, separated islands or mounds grow on the substrate and dislocations emerge where they meet. These are then overgrown by the deposited material. Diffusion of dislocations by concerted moves of the surrounding particles are highly improbable in the LJ-system and for the low temperatures considered here. We find a mean distance between dislocations very close to $1/\epsilon$ which directly reflects the *relative periodicity* of the two lattices involved.

For smaller misfits, one observes a more interesting evolution of the surface: initially, a pseudomorphic adsorbate film grows with the same mean lateral atomic distances $\bar{a}_{lat} \propto \sigma_s$ as in the substrate. At a rather well defined film thickness, misfit dislocations appear everywhere on the surface, which are later overgrown. Snapshots of the surface evolution in the vicinity of a single dislocation are shown in Figure 3 for $\epsilon = -5\%$.

In our most recent studies of the low misfit regime, we have slightly amended the model in comparison with Section 2. Deposited particles perform a so-called *downhill funneling* upon arrival at the surface: It is assumed that its kinetic energy enables an arriving atom to move to the lowest position in the vicinity of the deposition site. Similar incorporation effects, which are clearly not thermally activated, are discussed in [5] (this volume) and in greater detail in [1, 2]. The funneling process smoothens the surface by reducing the effect of the strong Schwoebel barrier in the system. It hence allows for the simulation of thicker films without a pronounced mound structure as, for instance, in Fig. 2. Note, however, that our findings are to a large extent robust with respect to such modifications.

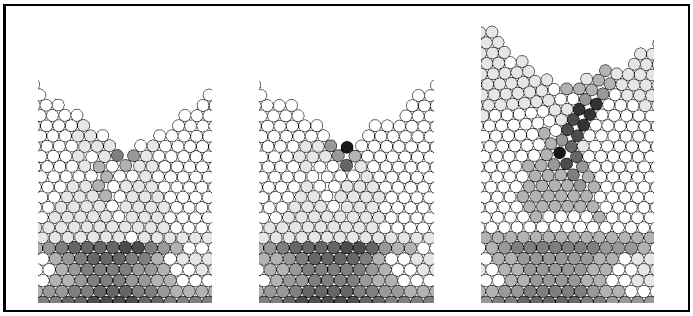


FIGURE 3. The emergence of a misfit dislocation in the model without downhill funneling [19] for $\epsilon = -5\%$, other details as in Fig. 2. The snapshots correspond to a mean film thickness of $12ML, 13ML$ and $18ML$, respectively.

For positive misfits the adsorbate is laterally compressed and it reacts by assuming a vertical lattice spacing $\bar{a}_\perp$ which is larger than in its undisturbed bulk. A simple consideration yields for small ϵ in the LJ-system a vertical spacing $\bar{a}_\perp^{const} \approx \bar{a}_{lat}\sqrt{3/4}(1+4/3\epsilon)$ of the atomic layers in the pseudomorphic film. After misfit dislocations have emerged, the adsorbate approaches its relaxed undisturbed bulk structure, as indicated by the decrease of $\bar{a}_\perp$ with the film thickness. Figure 4 shows the result of our simulations on average over 10 independent runs for system sizes of at least $L = 400$ and misfits in the range $1.4\% \leq \epsilon \leq 2.2\%$. The qualitative evolution of $\bar{a}_\perp$ agrees with novel measurements of this quantity in experimental studies of II-VI-semiconductor heteroepitaxy [29]. In a forthcoming publication the comparison with experimental data will be presented in greater detail.

Perhaps the most interesting result in this context concerns the *critical* film thickness h_c at which the dislocations appear in the system. In Fig. 4, it is marked by the deviation of $\bar{a}_\perp$ from its initial value. The rescaling of the thickness with $\epsilon^{-3/2}$ in Fig. 4 shows a relatively good collapse of the curves in the relevant phase of growth. It is by no means our intention to suggest that, here, a true *dynamical scaling law* exists as in, e.g., kinetic roughening [1, 2]. The small range of considered misfits would certainly not allow for such a claim. Nevertheless, our data is consistent with a critical thickness of the form

$$h_c \propto \epsilon^{-3/2}. \tag{3.1}$$

In the previous study of a slightly modified model we considered a different measure of the critical film thickness [19]. There, we found the same power law behavior for positive and negative misfits in a much wider range of misfits. Preliminary studies yield the same qualitative result for the model with other pair potentials in place of the Lennard-Jones interactions. Hence we believe that the observed dependence is robust with respect to details of the model and displays a certain degree of universality.

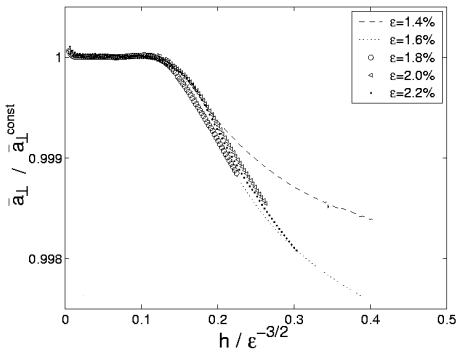


FIGURE 4. Dislocations: development of the vertical layer spacing in the model with *downhill funneling*, see text, with increasing film height for various values of the misfit. Results were obtained on average over 10 independent simulation runs and the spacing $\bar{a}_\perp$ is rescaled by its initial value. The scaling of the film thickness is according to Eq. (3.1) and results in a relatively good collapse of the curves close to the critical thickness.

Note that the power law behavior (3.1) disagrees with the results of energy or force balance considerations, as for instance the well-known and widely accepted relation derived by Matthews and Blakeslee [30]. One can argue, however, that the dislocation formation as observed here is a kinetic phenomenon far from equilibrium. Indeed, alternative approaches as suggested by Cohen-Solal and co-workers predict the power law dependence (3.1) for the critical thickness [31, 32]. Furthermore, experimental data for several IV-IV, III-V, and II-VI semiconductor systems shows very good agreement with the hypothesized power law [31, 32, 33].

In forthcoming investigations we will study the dependence of the surface evolution on the temperature and deposition rate. This should provide further evidence for the robustness of relation (3.1) and for the interpretation of misfit induced dislocation formation as an activated process.

4. Stranski-Krastanov like growth

Obviously, dislocations should dominate the strain relaxation in sufficiently thick films and for large misfits. In material systems with relatively small mismatch an alternative effect governs the initial growth of very thin films: Instead of growing layer by layer, the adsorbate aggregates in three-dimensional structures, allowing for partial relaxation. The term *3D-islands* is used to indicate that these structures are spatially separated. The effect is to be distinguished from the emergence of *mounds* due to the Ehrlich-Schwoebel instability [1, 2] which also occurs in homoepitaxy.

At least two distinct growth scenarios display 3D-island formation: In *Volmer-Weber* growth, the structures emerge immediately upon the substrate before the adsorbate even forms a closed layer [1]. The situation resembles the formation of non-wetting droplets of liquid on a surface. It is often observed in systems where adsorbate and substrate are fundamentally different, an example being Pb on a graphite substrate [1].

Here, we will focus on on the so–called *Stranski-Krastanov* (SK) growth mode, where 3D-islands are found upon a persistent pseudomorphic wetting-layer (WL) of adsorbate material [1, 6]. Most prominent examples for SK–systems are Ge/Si and InAs/GaAs where, as in almost all cases discussed in the literature, the adsorbate is under compression in the WL.

In order to avoid conflicts with more detailed or more restricted definitions of SK growth in the literature, we use the term *SK-like growth* here. It summarizes the following sequence of events during the deposition of a few monolayers (ML) of material:

1. Initial layer by layer growth of a pseudomorphic, compressed adsorbate WL.
2. The sudden appearance of 3D-islands, marking the so-called 2D-3D- or SK-transition at a *kinetic WL thickness* $h^*_{\rm WL}$.
3. Further growth of the 3D-islands, which is fed by additional deposition and by incorporation of surrounding WL atoms.
4. The observation of separated 3D-islands of similar shapes and sizes, on top of a WL with reduced *stationary thickness* $h_{\rm WL} < h^*_{\rm WL}$.

In order to avoid confusion, and since one might interpret our (1+1)-dim. model as a cross section of the full (2+1)-dim. picture, we will use the term 2D-3D-transition as usual throughout the following.

In SK growth a number of effects might play important roles, including the mixing interdiffusion of materials or the segregation of compound adsorbates. These effects are certainly highly relevant in many cases, see several contributions in [4] and [6]. However, SK–like growth is observed in a variety of material systems which may or may not display these specific features. For instance, intermixing or segregation should be irrelevant in the somewhat *exotic* case of large organic molecules like PTCDA deposited on a metal substrate. Nevertheless, this system shows SK–like growth according to the above definition [34].

This very diversity of SK–systems gives rise to the hope that this growth scenario might be explained in terms of a few basic mechanisms. Accordingly, it should be possible to capture and identify these universal features in relatively simple model systems without aiming at the reproduction of material specific details. This hope motivated the investigation of SK-growth in the frame of our off-lattice model.

An important modification beyond the description in Section 2 concerns the interlayer diffusion of adatoms. As argued above, the Ehrlich-Schwoebel effect would be much less pronounced in the physical $(2 + 1)$-dim. situation. In our investigation of the SK-like scenario we remove the ES-barrier for all interlayer

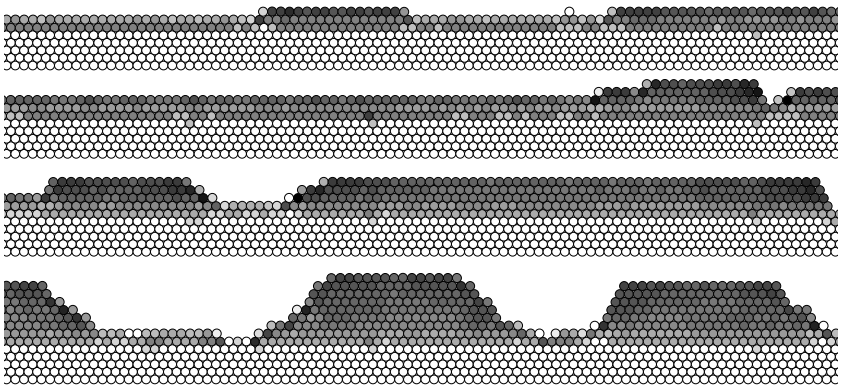


FIGURE 5. SK-like growth: A section of a simulated crystal with six layers of substrate as obtained for $\epsilon = +4\%$ and $R_d = 7.0ML/s$ at $T = 500K$ after deposition of (top to bottom) $1.5ML, 2.3ML, 3.0ML$ and $4.0ML$. In the second snapshot the critical WL thickness $h^*_{WL} \approx 2.3ML$ is reached and island formation sets in. Note how smaller islands grow and larger structures break up. Note also that WL particles contribute to the growth of islands. Eventually, the well separated structures are located on a stationary WL with, here, $h_{WL} \approx 1$. The darker a particle is displayed, the larger is the average distance from its nearest neighbors. White represents σ_s whereas σ_a corresponds to a dark grey on this scale.

diffusion events at terrace edges *by hand*. One motivation is the above mentioned over-estimation. More importantly, we wish to investigate strain induced island formation without interference of the ES instability. Note that the latter leads to the formation of mounds even in homoepitaxy [1, 2].

In order to favor the emergence of a wetting layer, we set $U_s > U_{as} > U_a$ in our model. As an example we have used $U_s = 1.0eV$, $U_a = 0.74eV$, and $U_{as} = 0.86eV$ accordingly. If not otherwise specified, we consider a positive misfit of $\epsilon = 4\%$ in the following. We have demonstrated before [19], cf. Section 3, that strain relaxation through dislocations is not expected for $\epsilon = 4\%$ within the first few adsorbate layers. Indeed, no misfit dislocations were observed in the simulations presented here.

In the simulation we realize a situation very similar to many experiments: a fixed amount of adsorbate material, corresponding to $4ML$, is deposited at a constant rate R_d. After deposition ends, we allow for a short relaxation period, in which atoms can still diffuse on the surface. Note however, that the essential surface properties are already determined during growth.

Our model displays a behavior along the lines of our operative definition of SK-like growth. The snapshots of an example simulation run in Figure 5 correspond precisely to the four stages outlined above, illustrating mpeg-movies of sample simulations are available at [35].

Several properties of surface diffusion in our model are discussed in [21] in greater detail. Here, we shortly summarize the essential features:

a) Adsorbate diffusion right on the substrate is relatively slow, due to the fact that U_{as} is quite large and satisfies $U_{as} > U_a$.
b) Adsorbate diffusion on a strained WL is relatively fast. The diffusion barrier decreases with the thickness, but essentially saturates at 3 or $4ML$ in our model, where the interaction with the substrate becomes negligible.
c) An adsorbate particle on top of an existing island is subject to a strong diffusion bias towards the island center. This result was already reported in [16]. The bias is due to the partial relaxation in the island and unrelated to the Ehrlich-Schwoebel effect, which has been eliminated in our model.

The first two effects, (a) and (b), clearly favor and stabilize the existence of a wetting layer. Qualitatively the same relation is obtained in experimental investigations of the Ge/Si system [36] and [6]. With the model parameters specified above we find an activation barrier of approximately $0.57eV$ for directly on the substrate and roughly $0.47eV$ for diffusion on the first wetting layer.

On the contrary, the diffusion bias (c) stabilizes existing islands by essentially confining adatoms to their top terraces. Of course this is the case for particles deposited onto the island. More importantly, we find a significant contribution of particles that jump upward, from the WL atop an island. The rate for such processes is quite small, generally, but becomes significant close to the SK-transition, see [21] for details.

In simulations with different deposition rates we observe that the kinetic WL thickness increases with R_d [20, 21]. If the formation of second or third layer nuclei by freshly deposited particles was the driving force, one would expect more frequent nucleation and an earlier 2D-3D-transition at higher growth rates. We conclude that, in the main, upward jumps trigger the SK-transition. Further evidence and a more detailed discussion of this important point is given in [21].

Our investigations suggest the following picture of the Stranski-Krastanov transition: The diffusion properties, (a) and (b), favor the formation of a wetting layer and stabilize it. As the film grows, strain accumulates in the film and upward hops from the WL become more probable. The precise spatial modulation of R_d in the film presumably determines the final island sizes and will be studied in forthcoming investigations. Once multilayer islands have emerged they are stabilized by the diffusion bias (c).

After the 2D-3D-transition, islands grow by incorporating newly deposited material, but also by consumption of the surrounding WL. Note that very large islands are observed to split by means of upward diffusion events onto their top layer, cf. Fig. 5. The migration of WL particles towards and onto the islands

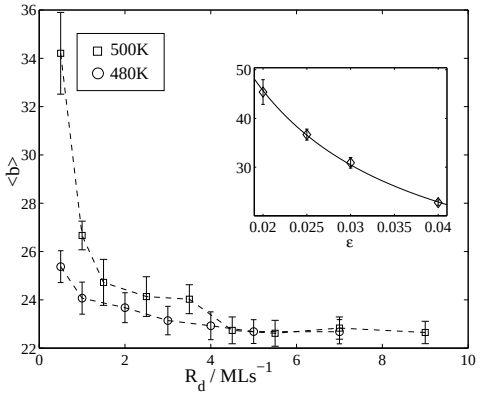


FIGURE 6. Average base size $\langle b \rangle$ of multilayer islands as a function of R_d at $T = 480$ and $T = 500K$, together with standard error bars. Results were obtained on average over 15 independent simulation runs. The inset shows the result for $T = 500K, R_d = 4.5ML/s$ and different misfit parameters, the solid line corresponds to $\langle b \rangle = 0.91/\epsilon$.

can well extend into the relaxation period after deposition ends. Eventually, a stationary WL thickness $h_{\mathrm{WL}} \approx 1$ is observed in our example scenario with $U_{as} \approx 0.86eV$. By increasing the strength of the adsorbate/substrate interaction we can achieve, e.g., $h_{\mathrm{WL}} \approx 2$ for $U_{as} \approx 2.7eV$, but it is difficult to stabilize a greater stationary thickness. This effect is related to the effective short range nature of the LJ-potential, which is very weak for distances larger than 3σ. With, e.g., long-range or multi-particle interactions, the model should yield greater WL thicknesses.

Finally, we discuss some properties of the emerging islands or SK-Dots. Figure 6 displays the average lateral size, measured as the number of particles in the island bottom layer. The results shown here were obtained at the end of a short relaxation period with $R_d = 0$. Whereas the mean values do not change significantly, fluctuations are observed to decrease in this phase.

We observe for two different temperatures that the island size decreases with increasing deposition rate. This is in accordance with several experimental observations [37]. However, the size becomes constant and independent of T for large enough deposition flux. A corresponding behavior is found for the island density and their lateral spacing, which hints at a considerable degree of spatial ordering [20, 21]. This saturation behavior further demonstrates the relevance of upward hops. Standard arguments [1, 2] show that a dominant aggregation of deposited particles on top terraces would yield an island density that continues to increase with R_d.

The inset in Fig. 6 displays the mean island size for $T = 500K$ and $R_d = 4.5ML/s$, i.e. in the saturation regime. Our result is consistent with a simple power

law of the form $\langle b \rangle \propto 1/\epsilon$. Very far from equilibrium, the only relevant length scale in the system appears to be, again, the relative periodicity $1/\epsilon$ of adsorbate and substrate lattice.

5. Summary and outlook

Despite its conceptual simplicity and the small number of parameters, our model reproduces several features of heteroepitaxial growth. Strain effects are incorporated in a natural fashion as they emerge directly from the interaction of particles. For instance, we have demonstrated that misfit dislocations appear in the system when the film thickness exceeds a characteristic value. This characteristic height displays a power law behavior on the lattice misfit.

We furthermore believe that, with appropriately chosen interaction parameters, our model is capable of reproducing the three essential growth modes: extended layer by layer growth (for very small misfits), Volmer-Weber for $U_{as} < U_a$ and, as demonstrated already, SK-growth for $U_{as} > U_a$. The small number of parameters should allow for determining the corresponding *phase diagram* of growth modes in the frame of our model system.

Besides the exploration of the available parameter space, we intend to extend the model conceptually in several directions. As just one example, intermixing and seggregation should be included to study the relevance of these effects in the Quantum Dot formation.

In order to test the potential universality of our findings, we will introduce different types of interactions in our model. Preliminary results for,e.g., Morse potentials [25] and modifications of LJ-potentials confirm our results in the context of dislocation formation. Ultimately, we will extend our model to the physical case of growth in $(2+1)$ dimensions and to realistic empirical potentials for metals or semi-conductors. As a first step, we are currently investigating the sub-monolayer regime in strained heteroepitaxy of fcc materials.

In a sense, the off-lattice KMC method provides a link between traditional, lattice based methods and Molecular Dynamics. Hence, it might play a significant role in the further development of the multiscale approach.

References

[1] A. Pimpinelli and J. Villain, *Physics of crystal growth.* Cambridge University Press (1998).

[2] T. Michely and J. Krug, *Islands, mounds and atoms. Patterns and Processes in Crystal Growth far from equilibrium.* Springer (2004).

[3] M.E.J. Newman and G.T. Barkema, *Monte Carlo Methods in Statistical Physics,* Oxford University Press (1999).

[4] M. Kotrla, N.I. Paanicolaou, D.D. Vvedensky, and L.T. Wille, *Atomistic Aspects of Epitaxial Growth.* Kluwer (2002).

[5] M. Biehl, *Lattice gas models of epitaxial growth and Kinetic Monte Carlo simulations.* This volume.

[6] B. Joyce, P. Kelires, A. Naumovets, and D.D. Vvedensky (eds.), *Quantum Dots: Fundamentals, Applications, and Frontiers.* Kluwer, to be published.

[7] D.C. Rapaport, *The Art of Molecular Dynamics Simulation.* Cambridge University Press (1995).

[8] M. Parrinello, *From silicon to RNA: The coming age of ab initio molecular dynamics.* Solid State Comm. **102** (1997) 107.

[9] K. Albe, this volume.

[10] L. Dong, J. Schnitker, R.W. Smith, D.J. Sroloviy, *Stress relaxation and misfit dislocation nucleation in the growth of misfitting films: a molecular dynamics simulation.* J. Appl. Phys. **83** (1997) 217.

[11] A.F. Voter, F. Montalenti, and T.C. Germann, *Extending the time scale in atomistic simulations of materials.* Annu. Rev. Mater. Res. **32** (2002) 321.

[12] A. Madhukar, *Far from equilibrium vapor phase growth of lattice matched III-V compound semiconductor interfaces: some basic concepts and Monte Carlo computer simulations.* Surf. Sci. **132** (1983) 344.

[13] K.E. Khor and S. Das Sarma, *Quantum Dot self-assembly in growth of strained-layer thin films: a kinetic Monte Carlo study.* Phys. Rev. **B 62** (2000) 16657.

[14] C.H. Lam, C.K. Lee, and L.M. Sander, *Competing roughening mechanisms in strained heteroepitaxy: A fast kinetic Monte Carlo study.* Phys. Rev. Lett. **89** (2002) 216102.

[15] M. Meixner, E. Schöll, V.A. Shchukin, and D. Bimberg, *Self-assembled quantum dots: crossover from kinetically controlled to thermodynamically limited growth.* Phys. Rev. Lett. **87** (2001) 236101.

[16] M. Schroeder and D.E. Wolf, *Diffusion on strained surfaces.* Surf. Sci. **375** (1997) 375.

[17] A.C. Schindler, *Theoretical aspects of growth in one and two-dimensional strained crystal surfaces.* Dissertation, Univeristät Duisburg (1999).

[18] A.C. Schindler and D.E. Wolf, *Continuous space Monte Carlo simulations in a model of strained epitaxial growth.* Unpublished, Universität Duisburg (1999) (available at http://www.comphys.uni-duisburg.de/MBE.html)

[19] F. Much, M. Ahr, M. Biehl, and W. Kinzel, *Kinetic Monte Carlo simulations of dislocations in heteroepitaxial growth.* Europhys. Lett. **56** (2001) 791–796.

[20] F. Much and M. Biehl, *Simulation of wetting-layer and island formation in heteroepitaxial growth.* Europhys. Lett. **63** (2003) 14–20.

[21] M. Biehl and F. Much, *Off-lattice Kinetic Monte Carlo simulations of Stranski-Krastanov-like growth.* In [6], in press (2004).

[22] F. Much, *Modeling and simulation of strained heteroepitaxial growth.* Dissertation Universität Würzburg (2003).

[23] J. Kew, M.R. Wilby, and D.D. Vvedensky, *Continuous-space Monte Carlo simulations of epitaxial growth.* J. Cryst. Growth **127** (1993) 508.

[24] H. Spjut and D.A. Faux, *Computer simulation of strain-induced diffusion enhancement of Si adatoms on the Si(001) surface.* Surf. Sci. **306** (1994) 233.

[25] F. Jensen, *Introduction to Computational Chemistry,* Wiley (1999).

[26] G.T. Barkema and N. Mousseau, *Event-based relaxation of continuous disordered systems.* Phys. Rev. Lett. **77** (1996) 4358.

[27] N. Mousseau and G.T. Barkema, *Traveling through potential energy landscapes of disordered materials: the activation relaxation technique.* Phys. Rev. **E 57** (1998) 2419.

[28] R. Malek and N. Mousseau, *Dynamics of Lennard-Jones clusters: A characterization fo the activation relaxation technique.* Phys. Rev. **E 62** (2000) 7723.

[29] A.S. Bader, W. Faschinger, C. Schumacher, J. Geurts, and L.W. Molenkamp, *Real-time in situ X-ray diffraction as a method to control epitaxial growth.* Appl. Phys. Lett. **82** (2003) 4684.

[30] J.W. Matthews and A.E. Blakeslee, *Defects in epitaxial multilayers.* J. Cryst. Growth **27** (1974) 118.

[31] G. Cohen-Solal, F. Bailly, and M. Barbé, *Critical thickness of zinc-blende semiconductor compounds.* J. Cryst. Growth **138** (1994) 138.

[32] F. Bailly, M. Barbé, and G. Cohen-Solal, *Setting up of misfit dislocations in heteroepitaxial growth and critical thickness.* J. Cryst. Growth **153** (1995) 153.

[33] K. Pinardi, U. Jain, S.C. Jain, H.E. Maes, R. Van Overstraeten, and M. Willander, *Critical thickness and strain relaxation in lattice mismatched II-VI semiconductor layers.* J. Appl. Phys. **83** (1998) 4724.

[34] L. Chkoda, M. Schneider, V. Shklover, L. Kilian, M. Sokolowski, C. Heske, and E. Umbach, *Temperature-dependent morphology and structure of ordered 3,4,9,10-perylene-tetracarboxylicacid-dianhydride (PCTDA) thin films on Ag(111)*, Chem. Phys. Lett. **371** (2003) 548.

[35] Illustrations and movies of our simulations are available at http://physik.uni-wuerzburg.de/~much{biehl}.

[36] V. Cherepanov and B. Voigtländer, *Influence of strain on diffusion at Ge(111) surfaces*, Appl. Phys. Lett. **81** (2002) 4745.

[37] J. Johansson and W. Seifert, *Kinetics of self-assembled island formation: Part I - island density*, J. Cryst. Growth **234** (2002) 132, and: *Part II - island size*, same volume, 139.

Acknowledgment

M.B. would like to thank the organizers and all participants of the MFO Mini-Workshop on *Multiscale Modelling in Epitaxial Growth* for the most stimulating atmosphere and many useful discussions. One of us (F.M.) was supported by the Deutsche Forschungsgemeinschaft.

Michael Biehl
University Groningen, Institute for Mathematics and Computing Science
P.O. Box 800, 9700 AV Groningen, The Netherlands
e-mail: `biehl@cs.rug.nl`

Florian Much
Universität Würzburg, Institut für Theoretische Physik
Am Hubland, D-97074 Würzburg, Germany
e-mail: much@physik.uni-wuerzburg.de

Christian Vey
Universität Würzburg, Institut für Theoretische Physik
Am Hubland, D-97074 Würzburg, Germany
e-mail: vey@physik.uni-wuerzburg.de